Asian Journal of Chemistry; Vol. 33, No. 3 (2021), 665-670

ASIAN JOURNAL OF CHEMISTRY

https://doi.org/10.14233/ajchem.2021.23052

Effect of Cu Doping on Structural and Dielectric Properties of $Pb_{1-x}Cu_x(Zr_{0.52}Ti_{0.48})O_3(PC_xZT)$ ($0 \le x \le 0.2$) Ceramics Prepared by Sol-Gel Method

M. AHABBOUD[1,*], T. LAMCHARFI[1,*], F. ABDI[1], N. HADI[1], F.Z. AJYAJE[1] and M. HADDAD[2]

[1]Signals, Systems and Components Laboratory (LSSC), Electrical Engineering Department, Faculty of Sciences and Technologies Fez, Imouzzer Road B.P. 2202, University Sidi Mohamed Ben Abdellah Morocco
[2]Spectrometry, Materials and Archaeomaterials Laboratory (LASMAR), Faculty of Sciences, Moulay Ismail University, Meknes, Morocco

*Corresponding author: E-mail: malikasmp2013@gmail.com; lamcharfi_taj@yahoo.fr

Received: 5 November 2020; *Accepted*: 29 January 2021; *Published online*: 16 February 2021; AJC-20266

In present work, the structural and dielectric properties of $Pb_{1-x}Cu_xZr_{0.52}Ti_{0.48}O_3$ (PC_xZT) ceramics where x = 0. 0.025, 0.05, 0.075, 0.10, 0.15 and 0.20 were studied. Powder of the compositions (PC_xZT) was obtained by sol-gel route, the powders were calcined at 700 ºC for 4 h and sintered at 1100 ºC for 4 h. X-ray diffraction analysis and Raman spectroscopy suggest the formation of mixed-phase of tetragonal and rhombohedral structure which was confirmed by Rietveld refinement. Dielectric measurements of the compounds were studied as a function of temperature (from room temperature to 420 ºC at different frequencies) and as a function of frequency (from 100 Hz to 2 MHz at different temperatures). The temperature variation of the real permittivity gives evidence of the ferroelectric phase transition as well as of the resonance behaviour also observed in the dielectric permittivity frequency-dependent variation.

Keywords: $Pb_{1-x}Cu_xZr_{0.52}Ti_{0.48}O_3$ ceramics, Dielectric properties, Raman spectroscopy, Ceramics, Reitveld refinement.

INTRODUCTION

Ferroelectric materials are known for many years. They are the materials with reversible spontaneous polarization [1]. In recent years, there are several perovskites which have been reported as ferroelectrics like strontium titanate ($SrTiO_3$), barium titanate ($BaTiO_3$), lead titanate ($PbTiO_3$), lead zirconate ($PbZrO_3$), calcium titanate ($CaTiO_3$), lithium tantalate ($LiTaO_3$) and lead zirconate titanate ($PbZr_{1-y}Ti_yO_3$) [2-5]. Lead zirconate titanate $Pb(Zr_{1-y}Ti_y)O_3$ has been considered to be one of the most important members of the perovskite family, as they exhibits very interesting electrical and electromechanical properties. Additionally, they also have high pyroelectric coefficient, high transition temperature and the maximum electromechanical constants and widely applied in several industrial sectors [6-8]. The $PbZr_{0.52}Ti_{0.48}O_3$ (PZT) is considered one of the best ceramics, which is attributed due to the coexistence of rhombohedral (*R*3*m*) and tetragonal (*P*4*mm*) phases, similarly $Pb(Zr_{1-y}Ti_y)O_3$ exhibits the maximum electrical and dielectric properties, as $y = 0.48$, which is near morphotropic phase boundary [7]. Normally these materials can be prepared by different methods, however, chemical coprecipitation method [9] is considered vastly as most convenient, since it is found that the PZT ceramics crystallize in the tetragonal and monoclinic phases [10]. The homogeneous precipitation that the main peaks of PZT area tetragonal perovskite structure. While Ramana *et al.* [11] obtained these ceramics by mechanical alloying and studied electrical and mechanical properties of PZT as a function of temperature, they indicated also that most of the XRD peaks of PZT were indexed in tetragonal and rhombohedral phases.

In all of these structural studies, problems typically encountered the loss of lead enormously due to the volatility of PbO at elevated temperatures. In addition, the structural and dielectric properties of Cu doped PZT ceramics were less investigated. In present work, a new $Pb_{1-x}Cu_x(Zr_{0.52}Ti_{0.48})O_3$ (PC_xZT) ceramics ($0 \le x \le 0.2$) was prepared by the sol-gel route. The X-ray diffraction techniques, Raman spectroscopy and dielectric measurements of PC_xZT ceramics were investigated. Moreover, based on the experimental results, the effect of Cu doped PZT nanoparticles were discussed.

EXPERIMENTAL

The (PC_xZT) nanopowders ($x = 0, 0.025, 0.05, 0.075, 0.10, 0.15$ and 0.20) were synthesized by sol-gel route. The PC_xZT samples are prepared of starting precursors such as lead(II) acetate trihydrate [$Pb(CH_3COO)_2{\cdot}3H_2O$] 99% purity, zirconium acetate [$Zr(CH_3COO)_4$] 99.9% purity, titanium isopropoxide [$Ti(OCH(CH_3)_2)_4$] 99.9% purity and copper(II) acetate monohydrate [$Cu(CH_3COO)_2{\cdot}H_2O$] 98% purity.The acetates were dissolved in distilled water to obtain solution 1. Then, solution 1 was mixed with stoichiometric amounts of sol [$Ti(OCH(CH_3)_2)_4$] to obtain solution 2. Solution 2 was stirred for 1 h to get a homogenous sol. After, the sol was dried at 80 ºC to remove water forming a xerogel and then a gel. The powders obtained from PC_xZT was calcined at 700 ºC for 4 h. The calcined powders were mixed with the polyvinyl alcohol as a binder and pressed into pellets of diameter 12 mm and thickness 2 mm. The pellets were placed in the rich PbO atmosphere using $PbTiO_3$ as a spacer powder to compensate for the loss of lead that probably evaporated during heat treatment [11,12]. These pellets were then sintered at 1100 ºC for 4 h with a heating rate of 5 ºC/min. The phase structure of PC_xZT powders was determined by X-ray diffraction measurements with an (XPERT-PRO diffractometer system) with CuK_α radiation and ($\lambda = 1.5406$ Å). Data were registered at room temperature in the angular range 20-80º in 2θ with a step of 0.04º. The lattice parameters were collected from the Rietveld method using Fullprof software of the experimental diffraction data. Raman spectroscopy was measured at room temperature and used to study the relationship between Raman lines and different types of atomic motions of PC_xZT ceramics. The dielectric properties as a function of frequency and temperature were investigated using an Agilent impedance analyzer (Agilent E4980A) in the frequency range from 100 Hz to 2 MHz and a wide range of temperatures (50-420 ºC).

RESULTS AND DISCUSSION

The X-ray diffraction patterns at room temperature of PC_xZT ($x = 0, 0.025, 0.05, 0.075, 0.10, 0.15$ and 0.20) samples annealed at 700 ºC for 4 h are shown in Fig 1a. The XRD of pure and Cu doped PZT shows a pure perovskite phase, except at $x = 0.15$, it is observed a small peak increased with the increase of copper in the PZT perovskite. For more clearly, the zoom of the (110) peak is shown in Fig 1b, where the peak shifted to high angles for $x = 0.025$ and to lower angles for $0.05 \leq x \leq 0.10$. This change is probably due to two possibilities (i) substitution of Pb^{2+} by Cu^{2+} and (ii) substitution of Zr^{4+}/Ti^{4+} by Cu^{2+}. These results are consistent with the results reported in the literature, where researchers studied different properties by modifying the Pb^{2+} side by Mg^{2+} in PZT ceramics [13]. The second possibility is confirmed by Khorrami *et al*. [14], where the substitutions of Ti^{4+} by Zn^{2+}, Mg^{2+} and Mn^{2+} ions were investigated. They reported that doping with Mn^{2+} is responsible to the shift to the higher angles; whereas the substitution of Zn^{2+} and Mg^{2+} effect the shift to lower angles which is due to a decrease of the d-spacing of the planes and high ionic radius of $r_{(Zn \text{ and } Mg)} > r_{Ti}$), respectively [14].

An analysis of PC_xZT ceramic was carried out by Rietveld refinement using the Fullprof program package. The pseudo-Voigt peak shape function option was chosen to define the peak profiles and the background was estimated by linear interpolation between fixed values. Rietveld analysis confirms the match of data observed with *R*3*m* and *P*4*mm* space groups, which are related to rhombohedral and tetragonal structures respectively (Fig. 2). Moreover, the small peak observed in Fig. 1 is attributed to copper oxide. The lattice parameters, the quality of fit (χ^2) and R-factors (R_p, R_{wp}, R_{exp}) values calculated by Rietveld refinement are given in Table-1. For all the samples, the χ^2, R_p, R_{wp}, R_{exp} values revealed in the allowed terms; while with the increasing copper content, the fluctuation in lattices

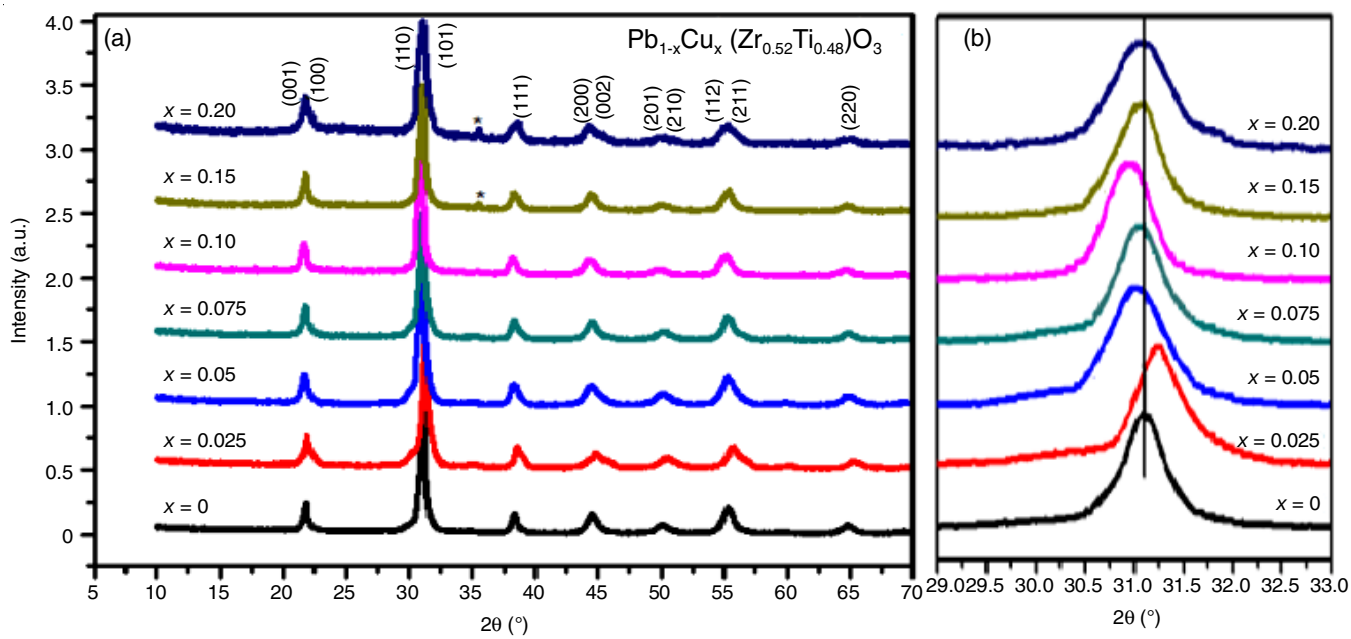

Fig. 1. (a) XRD patterns and (b) Zoom of the peak (110) in the 2θ range of 29-33° of PC_xZT samples calcined at 700 °C for 4 h

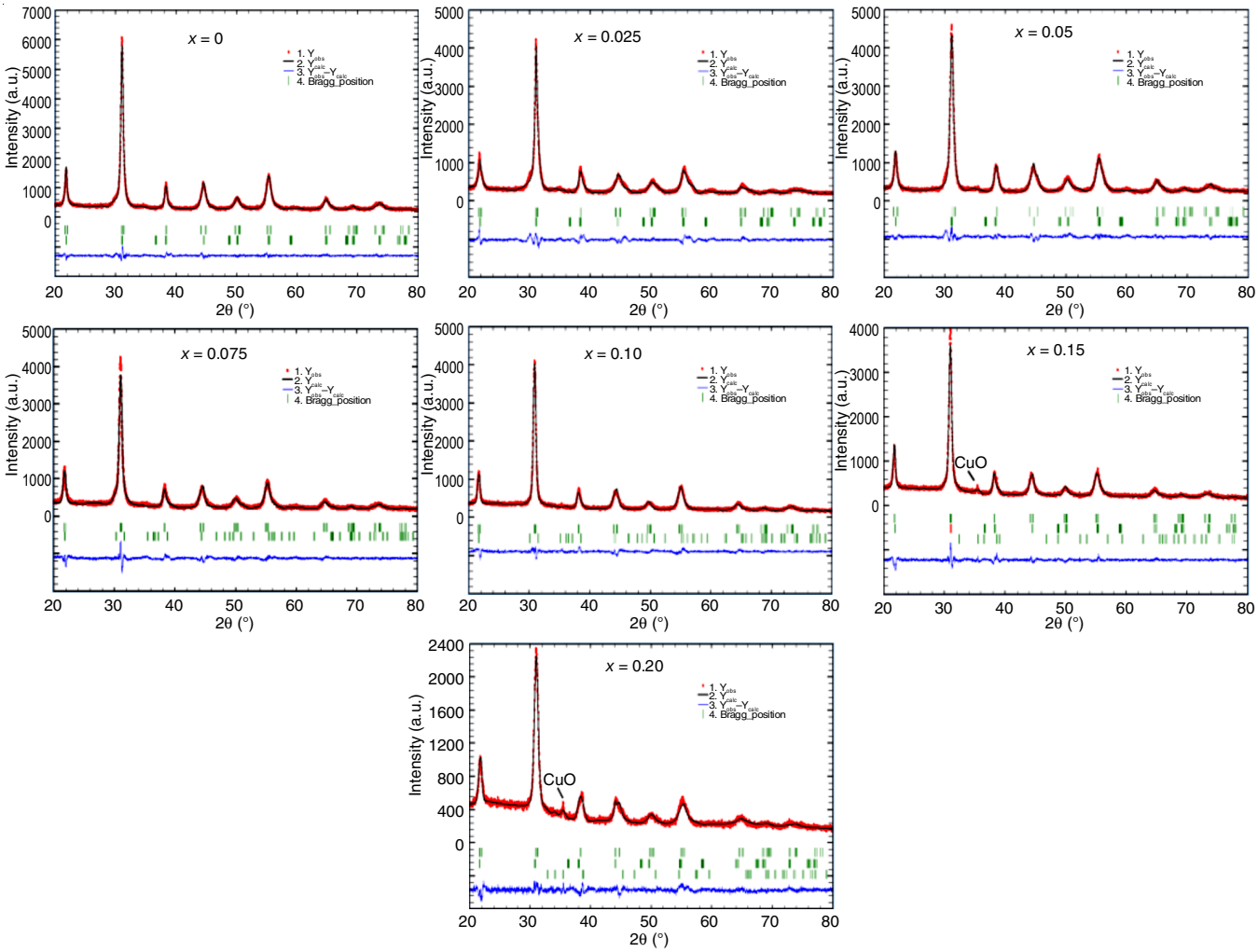

Fig. 2. Rietveld refined the XRD pattern of $Pb_{1-x}Cu_xZr_{0.52}Ti_{0.48}O_3$ samples calcined at 700 °C for 4 h

TABLE-1
LATTICE PARAMETERS (a,b), VOLUME, R_p, R_{wp}, R_{exp} AND χ^2, VALUES FOR THE STRUCTURES OF PC_xZT CERAMICS FOR $0 \le x \le 0.2$

x	Lattice parameters (a,b) and V (Å)		R_p (%)	R_{wp}	R_{exp}	χ^2
	Rhombohedral	Tetragonal				
0.000	a = 5.7510; c = 14.1262	a = 4.0402; c = 4.1098	3.92	4.97	4.70	1.12
0.025	a = 5.7611; c = 14.0768	a = 4.0348; c = 4.1044	6.50	8.33	5.50	2.30
0.050	a = 5.7289; c = 14.1143	a = 4.0010; c = 4.1157	5.03	6.50	5.06	1.65
0.075	a = 5.7553; c = 14.1792	a = 4.0143; c = 4.1430	6.40	7.97	5.47	2.12
0.100	a = 5.6812; c = 14.9518	a = 4.0761; c = 4.1220	5.24	6.79	5.58	1.48
0.150	a = 5.7652; c = 14.0799	a = 4.0669; c = 4.1032	4.93	6.34	5.46	1.35
0.200	a = 5.8162; c = 14.1804	a = 4.0524; c = 4.1099	4.73	6.22	5.48	1.29

parameter values (a and c) is perhaps due to the compositional fluctuations, and substitutional disordering in the arrangement of cations in one or more crystallographic sites (Pb^{2+}, Zr^{4+} or Ti^{4+}) of the structure. These results are confirmed by Sanchez-Caceres *et al*. [15]. Thus, the R_p, R_{wp} and R_{exp} values for all the samples are less than 6.50, 8.33 and 5.58, respectively. Additionally, the change of chi-squared (χ^2) is between 1.12 and 2.30 with the variation of copper content.

Raman spectra of PC_xZT solid solution for different concentration (x = 0.00, 0.025, 0.05, 0.075, 0.10, 0.15 and 0.20) at room temperature in the wavenumber range of 1000-100 cm^{-1} are shown in Fig. 3. For pure PZT (x = 0.00), in the frequency range from 100 to 800 cm^{-1}, the typical 3A1 + B1 + 5E modes in Raman peaks can be clearly identified, with eight main peaks: 203.63; 274.39; 331.23; 507.36; and 552.22; 597.07; 717.72; and 775.81 cm^{-1}, corresponding to the E(2TO), E(silent) + B1, A1(2TO), E(3TO), E(4TO), A1(3TO), E(4LO), and A1(3LO) modes [16], respectively. The E+B1 (silent) mode confirms the existence of rhombohedral and tetragonal structure [17]. The modes (TO3) observed at around 507.36 is assigned to (O–Ti–O) stretching symmetric vibrations of octahedral [TiO_6] clusters [18]. The obtained values of the pure sample are in good agreement with Buixaderas *et al.* [19] and Deluca *et al.* [20]. For Cu-doped PZT samples, similar peaks were observed,

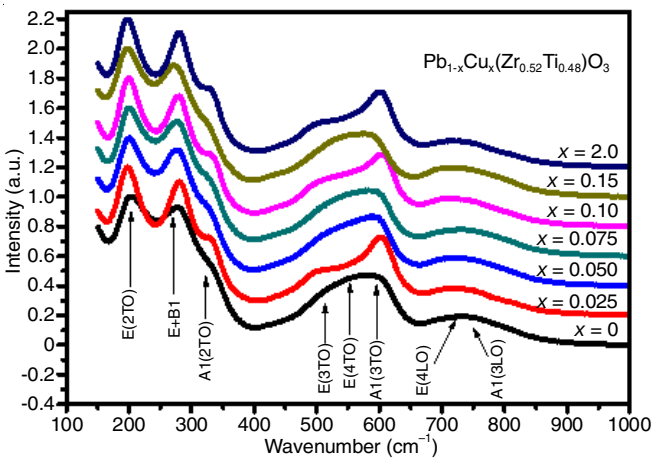

Fig. 3. Raman spectra of PC_xZT samples calcined at 700 °C for 4 h

but the intensity of these peaks is changed with increasing Cu content. Indeed, the change in different peaks of the Raman spectra indicates the structural modification caused by the substitution of Pb^{2+}, Zr^{4+} or Ti^{4+} by Cu^{2+}, which confirmed the shifts of the peak (110) and the fluctuation of lattice parameters observed in XRD. These results are consistent with the results reported in the literature [21].

Dielectric properties: Fig. 4 shows the variation of dielectric constant as a function of temperature at different frequencies (low frequency < 1 MHz) for all the PC_xZT nanoparticles with x = 0.0, 0.025, 0.05, 0.075, 0.10, 0.15 and 0.20. For the pure PZT, it is observed that the dielectric constant increases with increasing temperature and reach a maximum value at Curie temperature T_c = 410 ºC followed by a decrease. The observed dielectric behaviour is corresponding to the ferroelectric-to-paraelectric phase transition [22]. Similar behaviour is found for Cu doped PZT samples, and the phase transition shifted to the higher temperature with the increase of Cu content up to x = 0.10 then it shifted to the lower temperature, this is attributed to the disorder in the arrangement of cation at A-site which is occupied by Pb^{2+} or B-site occupied by (Zr^{4+}/Ti^{4+}) with Cu^{2+} additive. Besides, the dielectric constant maximum value of the PC_xZT ceramics decreases with the increase of Cu substitution up to x = 0.05 (ε is approximately 3230 at 50

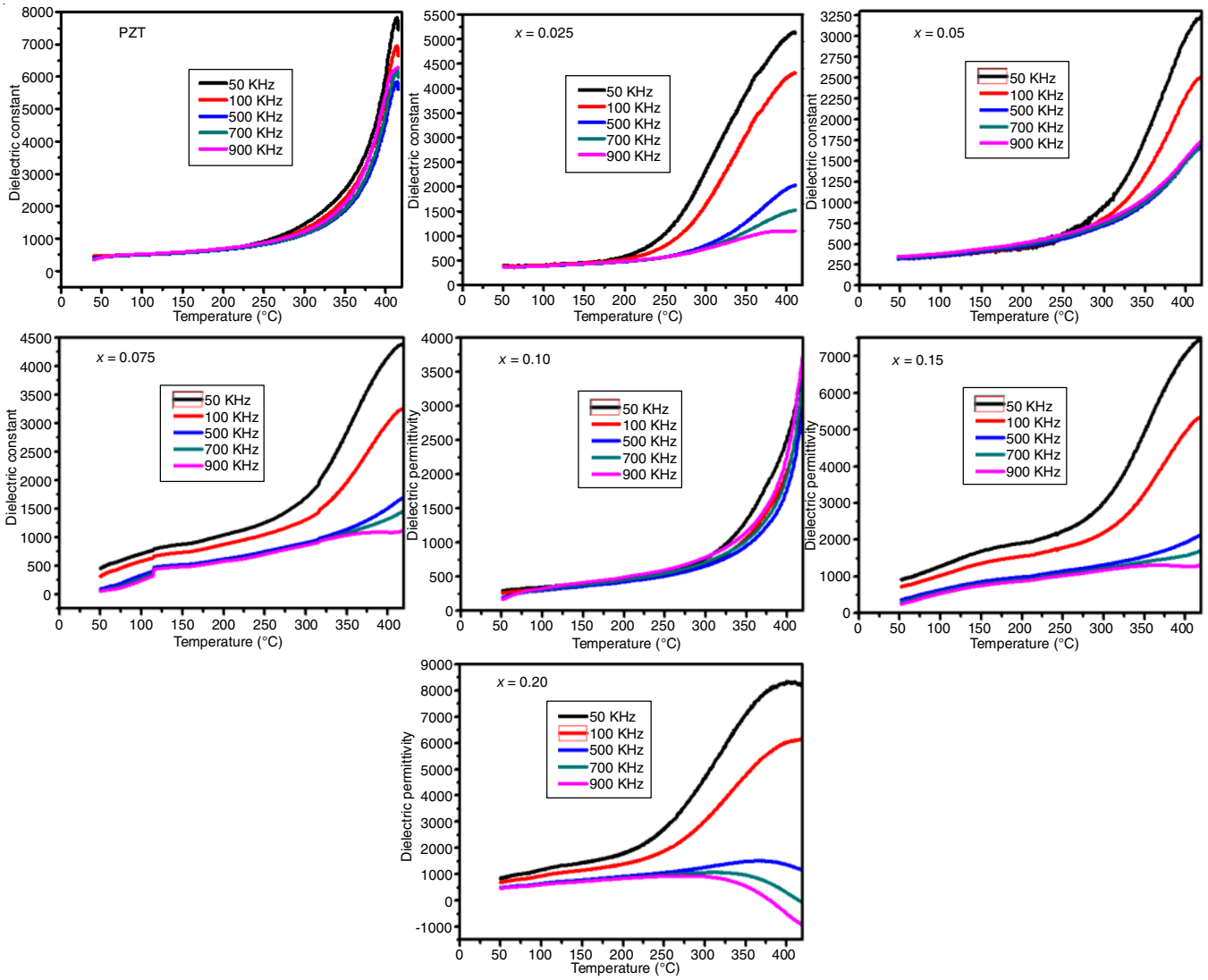

Fig. 4. Temperature-dependent dielectric constant of PC_xZT ceramics at different frequencies (f) < 1 MHz

KHz) then increases up to 8500 at 50 KHz for $x = 0.20$. The literature reports, for concentrations $x \leq 0.03$, that doping with materials like copper decreases the dielectric constant [12]. Fig. 5 shows the behaviour of the dielectric constant of studied ceramics ($x = 0.0$, 0.05 and 0.10) as a function of temperature at higher frequencies (f > 1 MHz). Moreover for pure PZT, when the frequency increases, the permittivity maximum value ε_{rmax} decreases and the maximum temperature T_m shifts towards lower temperatures. This behaviour is due to the dielectric resonance phenomena [23,24]. A similar evolution of dielectric permittivity as pure PZT was also observed for Cu doped PZT samples. The permittivity maximum value ε_{max} and T_m decrease with increasing Cu content up on $x = 0.05$ and then increases until $x = 0.10$, indicating the effect of Cu^{2+} doping on dielectric proprieties of PC_xZT ceramics (Table-2).

TABLE-2
T_m AND ε_{rmax} VALUES AT DIFFERENT FREQUENCIES OF PC_xZT CERAMICS

Freq. (MHz)	x = 0.00		x = 0.05		x = 0.10	
	T_m (°C)	ε_r (T_m)	T_m (°C)	ε_r (T_m)	T_m (°C)	ε_r (T_m)
1.0	405	5887	425	1805	418	3469
1.4	377	4636	396	1603	388	2344
1.8	346	3704	352	1516	346	1918
2.0	327	3308	330	1546	325	1732

The dielectric constant of PC_xZT composites ($x = 0.0$, 0.05 and 0.10) were investigated at different temperatures (120-400 ºC) as a function of frequency in the range of 100 Hz to 2 MHz. Fig. 6 shows that for $x = 0.00$, the dielectric constant increases with the increase in temperature and achieved the maximum value ε_{rmax}. From this maximum, the spectrum of ε_r decreases and goes through a minimum then increases again. It reveals that the maximum dielectric constant ε_{rm} increases with further increase in temperature and moves towards low frequencies. This phenomenon is due to the dielectric resonance. This evolution of ε_r with frequency variation is in good agreement with many reported works [24,25]. Furthermore, the values of resonance frequency (maximum value) were found to increase for $x = 0.05$ and decreases for $x = 0.10$. Besides, the permittivity maximum value ε_{rmax} decreases for $x = 0.05$ and increases for $x = 0.10$. The same evolution is found in case of the dielectric constant as a function of the temperature at higher frequencies.

Conclusion

In this study, $Pb_{1-x}Cu_x(Zr_{0.52}Ti_{0.48})O_3$ nanoparticles have been successfully synthesized *via* a sol-gel process with different compositions ($x = 0.0$, 0.025, 0.05, 0.075, 0.10, 0.15 and 0.20) using $Pb(Zr,Ti)O_3$ template powders obtained by mixed metal acetates. The X-ray Rietveld technique and Raman analysis confirmed the coexistent of rhombohedral and tetragonal phases. The evolution of the permittivity as a function of temperature shows that the incorporation of Cu content shifts the phase transition to the higher temperature. Besides, the permittivity maximum value decreases for $x = 0.05$ and increases for $x = 0.10$ in case of variation of the dielectric constant as a function of temperature and frequency.

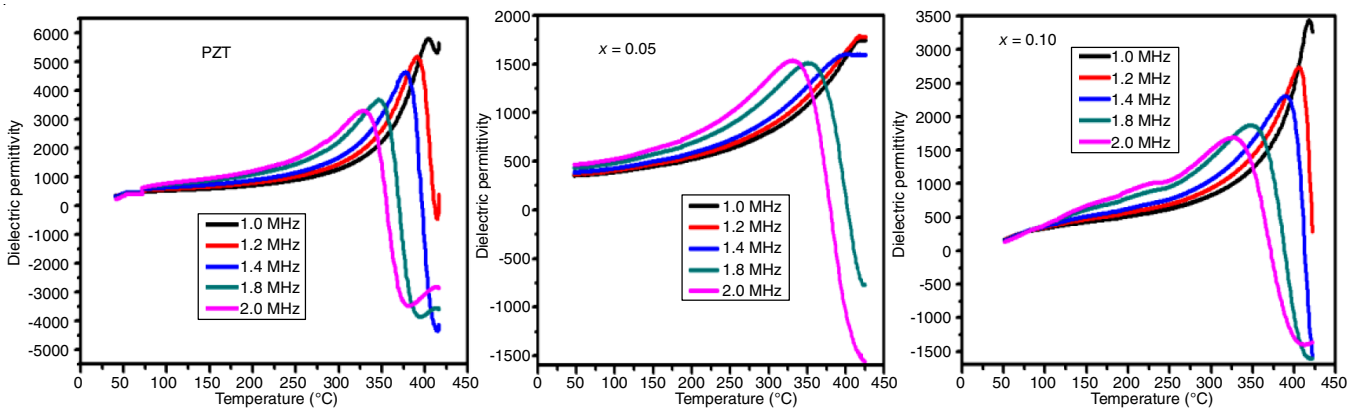

Fig. 5. Temperature-dependent dielectric constant of PC_xZT ceramics at different frequencies (f) > 1 MHz

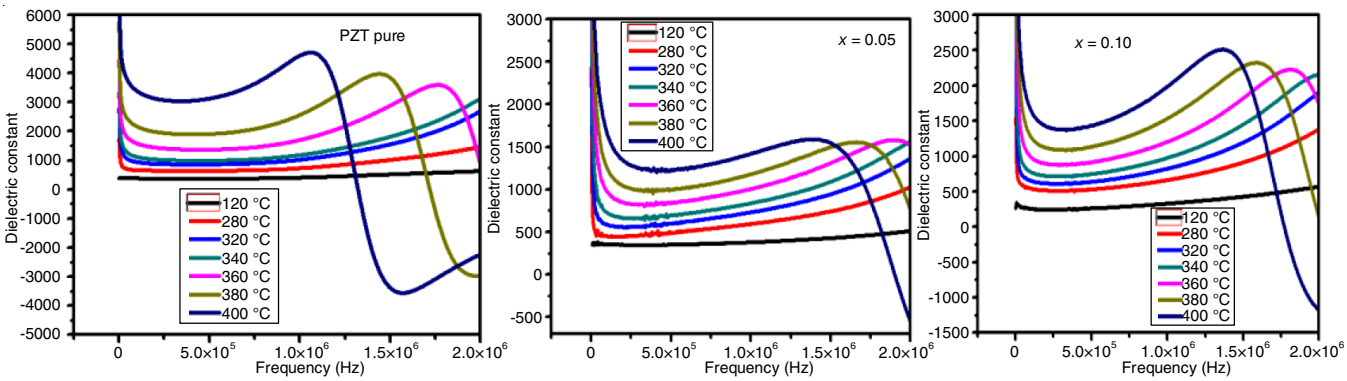

Fig. 6. Frequency-dependent dielectric constant of PC_xZT ceramics at different temperatures

CONFLICT OF INTEREST

The authors declare that there is no conflict of interests regarding the publication of this article.

REFERENCES

1. S. Nayak, T.K. Chaki and D. Khastgir, *J. Ceramics Int.*, **42**, 14490 (2016); https://doi.org/10.1016/j.ceramint.2016.06.056
2. S.H. Han, W.S. Ahn, H.C. Lee and S.K. Choi, *J. Mater. Res.*, **22**, 1037 (2007); https://doi.org/10.1557/jmr.2007.0122
3. H. Liu and B. Dkhil, *J. Z. Kristallogr.*, **226**, 163 (2011); https://doi.org/10.1524/zkri.2011.1336
4. Y. Xu, C.H. Cheng and J.D. Mackenzie, *J. Non-Cryst. Solids*, **176**, 1 (1994); https://doi.org/10.1016/0022-3093(94)90205-4
5. J. Ravez, G.T. Joo, M. Dong and J.M. Reau, *J. Phys. Stat. Sol.*, **146**, K71 (1994); https://doi.org/10.1002/pssa.2211460249
6. M. Kumar, S. Shankar, S. Kumar, O.P. Thakur and A.K. Ghosh, *J. Mater. Sci. Mater. Electron.*, **27**, 6849 (2016); https://doi.org/10.1007/s10854-016-4637-8
7. C.A. Oliveira, E. Longo, J.A. Varela and M.A. Zaghete, *Ceramics Int.*, **40**, 1717 (2014); https://doi.org/10.1016/j.ceramint.2013.07.068
8. R.G. Polcawich and J.S. Pulskamp, eds.: H. Bhugra and G. Piazza, Piezoelectric MEMS Resonators, RDRL-SERL, 2800 Powder Mill Road, Adelphi, MD 20783, USA, pp 39-71 (2017).
9. Ragini, R. Ranjan, S.K. Mishra and D. Pandey, *J. Appl. Phys.*, **92**, 3266 (2002); https://doi.org/10.1063/1.1483921
10. A. Mandal, D. Ghosh, A. Malas, P. Pal and C.K. Das, *J. Eng.*, **2012**, 391083 (2012); https://doi.org/10.1155/2013/391083
11. M.V. Ramana, M.P. Reddy, N.R. Reddy, K.V. Siva Kumar, V.R.K. Murthy and B.S. Murty, *J. Nanomater.*, **2010**, 7830438 (2010); https://doi.org/10.1155/2010/783043
12. K.L. Yadav and P. Sharma, *Indian J. Eng. Mater. Sci.*, **15**, 61 (2008).
13. S.K. Pradhan, A. Kumar, P. Kour, R. Pandey, P. Kumar, M. Kar and A.N. Sinha, *J. Mater. Sci. Mater. Electron.*, **29**, 16842 (2018); https://doi.org/10.1007/s10854-018-9779-4
14. Gh.H. Khorrami, A. K. Zak, A. Kompany and R. Yousefi, *Ceram. Int.*, **38**, 5683 (2012); https://doi.org/10.1016/j.ceramint.2012.04.012
15. J.A.S. Caceres, C.A.C. Passos, J.V.S. Chagas, R.C. Barbieri and R.T. Corteletti, *Mater. Res.*, **22**, e20190123 (2019); https://doi.org/10.1590/1980-5373-mr-2019-0123
16. A.G.S. Filho, K.C.V. Lima, A.P. Ayala, I. Guedes, P.T.C. Freire, F.E.A. Melo, J.M. Filho, E.B. Araujo and J.A. Eiras, *Phys. Rev. B*, **66**, 1321071 (2002); https://doi.org/10.1103/PhysRevB.66.132107
17. P. Kour, S.K. Pradhan, P. Kumar, S.K. Sinha and M. Kar, *AIP Conf. Proc.*, **1728**, 020490 (2016); https://doi.org/10.1063/1.4946541
18. M. Mesrar, T. Lamcharfi, N. Echatoui, F. Abdi and A. Harrach, *Asian J. Chem.*, **30**, 1012 (2018); https://doi.org/10.14233/ajchem.2018.21116
19. E. Buixaderas, M. Berta, L. Kozielski, and I. Gregora, *Phase Transac.*, 84 528 (2011); https://doi.org/10.1080/01411594.2011.552049
20. M. Deluca, H. Fukumura, N. Tonari, C. Capiani, N. Hasuike, K. Kisoda, C. Galassi and H. Harima, *J. Raman Spectrosc.*, **42**, 488 (2011); https://doi.org/10.1002/jrs.2714
21. H. Li, J. Liu, H. Yu and Sh. Zhang, *J. Adv. Ceram.*, **3**, 177 (2014); https://doi.org/10.1007/s40145-014-0106-0
22. T. Lamcharfi, Ph.D. Thesis, Elaborationpar voie hydrothermale et caractérisation des ceramiques ferroelectriques de type perovskite PZT dopées au lanthane $Pb_{1-y}La_y(Zr_xTi_{1-x})O_3$, Université de Bordeaux I, France (2005).
23. A. Elbasset, F. Abdi, T. Lamcharf, S. Sayouri, L.H. Omari, P. Bourson, A. Salhi and A. Elghandouri, *Int. Rev. Physiol.*, **8**, 5 (2014).
24. M. Mesrar, T. Lamcharfi, N.S. Echatoui, F. Abdi, F.Z. Ahjyaje and M. Haddad, *Mediterr. J. Chem.*, **8**, 198 (2019); https://doi.org/10.13171/mjc8319050908mm
25. A. Peláiz-Barran and J.D.S. Guerra, eds.: I. Coondoo, Ferroelectrics, chap. 10 (2010).